

**A. Kurz, S. Grundmann, C. Tropea**

(Technische Universität Darmstadt)

**M. Forte, A. Seraudie, O. Vermeersch,**

**D. Arnal**

(Onera)

**N. Goldin, R. King**

(Technische Universität Berlin)

E-mail: kurz@csi.tu-darmstadt.de,

maxime.forte@onera.fr

# Boundary Layer Transition Control using DBD Plasma Actuators

This paper presents experimental and numerical investigations dealing with 2D boundary-layer transition control on an Onera-D airfoil using Dielectric Barrier Discharge actuators. These actuators generate a non-thermal surface discharge, which induces a momentum addition tangentially and close to the wall. In this case, the ability of this kind of plasma actuators to delay transition has been assessed using both steady and unsteady modes of actuation. On the one hand, wind tunnel investigations are conducted, as well as linear stability analyses, in order to study the effect of a steady operated DBD actuator on boundary-layer stabilization. The results show a maximum transition delay of about 35% of the chord for low free-stream velocity ( $U_\infty = 7$  m/s). On the other hand, an experiment has been performed using the unsteady force produced by the DBD actuator, to achieve Active Wave Cancellation in a direct frequency mode. With the help of a closed loop control system, a significant transition delay has been achieved by damping artificially introduced TS waves for free-stream velocities up to  $U_\infty = 20$  m/s. This work has been conducted within the framework of the PlasmAero project, funded by the European Commission.

## Introduction

Plasma actuators for flow control applications have been studied for more than a decade now. Basically, these actuators can be sorted into two groups, depending on the kind of plasma that is generated: non-thermal plasma or thermal plasma. Thermal plasma actuators are based on the generation of an equilibrium discharge, in order to locally increase the pressure and the temperature of the surrounding gas. For example, Plasma Synthetic Jet (PSJ) actuators generate a spark discharge inside a small cavity having a pinhole exit at the wall. The pressure increase inside this cavity induces a wall-normal jet, which acts on the boundary layer as a vortex generator. These actuators have shown promising results in controlling several academic aerodynamic configurations, such as compressible jets or incompressible separated boundary layers [4], [12]. Non-thermal plasma actuators, like Dielectric Barrier Discharge (DBD) [19] or Corona Discharge [14], are based on the generation of a non-equilibrium surface discharge, which induces a body force parallel to the wall (called ionic wind) inside the boundary layer. This kind of actuator has been widely characterized in quiescent air for different ambient conditions. Moreover, many investigations have shown their ability to control airflows around different kinds of bodies: flat plates, cylinders and airfoils. Most of

these studies are reported in detailed reviews [2], [5], [15]. The work presented in this paper has been performed within the framework of the PlasmAero project, funded by the European Commission, for which the main objective is to assess the ability of plasma actuators to control airflows, in order to reduce the environmental impact of air transport. One possible way to reduce aircraft fuel consumption is to delay boundary-layer transition on wing profiles, in order to reduce skin friction drag. Basically, two approaches are possible to achieve this goal on a 2D boundary-layer transition: on the one hand, steady actuation is used to modify the mean velocity profile, in order to make the boundary layer more stable. Different kinds of actuation have shown good results using this approach, like for instance steady suction. On the other hand, unsteady actuation is used to act (or counteract) directly on the instabilities growing within the boundary layer, the well-known Tollmien-Schlichting (TS) waves, which lead to turbulence for low disturbance level airflow. This approach is called Active Wave Cancellation (AWC). The goal of this study is to show the ability of a DBD plasma actuator to delay transition on an airfoil by means of either steady or unsteady actuation, as this actuator is able to induce either continuous or unsteady momentum addition to the boundary layer, depending on the electrical parameters of the high-voltage signal.

## Experimental setup

These experiments have been conducted in the subsonic open-return “Juju” wind tunnel located at the research facilities of Onera Toulouse. It features a low turbulence level  $0.5 \times 10^{-3} < Tu < 0.5 \times 10^{-2}$  depending on the free-stream velocity, which ranges from 5 to 75 m/s. This facility operates at ambient conditions and is well suited for transition experiments. As illustrated in figure 1, a two-dimensional model based on an Onera-D symmetric profile, having a chord length of  $c = 0.35$  m, is mounted horizontally in the test-section of the wind tunnel.

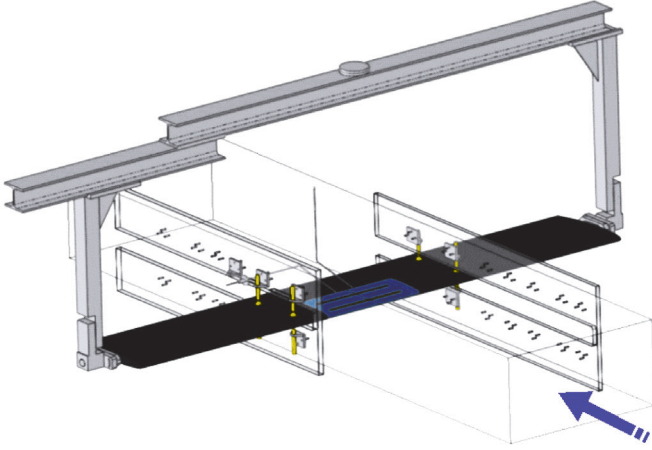


Figure 1 – Two-dimensional model of the Onera-D airfoil mounted inside the wind tunnel

The angle of attack can be adjusted between  $\alpha = -8^\circ$  and  $\alpha = +3^\circ$ , in order to modify the pressure gradient and thus the natural transition location. Additionally, the model is equipped with 15 pressure taps on the upper side.

The DBD plasma actuator used during this experiment consists of a 5 mm-thick dielectric layer (blue insert in figures 1 and 2) made of Lab850 material, placed at the leading edge region and matching the model shape. This insert allows the model to be outfitted with the desired number of DBD actuators, adhering electrodes asymmetrically on both sides of the dielectric material. For example, figure 2 shows one single DBD actuator located at  $x/c = 10\%$  (the downstream edge of the air-exposed electrode is taken as the location reference).

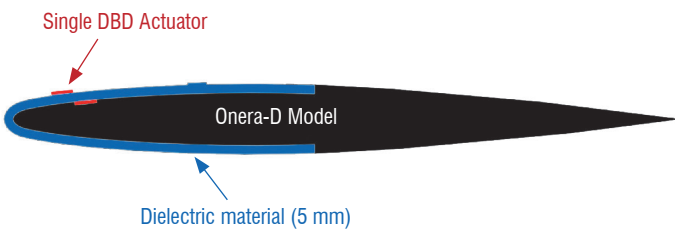


Figure 2 – Cross-sectional view of the Onera-D wing model equipped with one DBD actuator

The electrodes are 30 cm-long in spanwise direction and made of copper tape. The air-exposed electrodes are connected to a TREK power amplifier (model 30/20,  $\pm 30$  kV, 20 mA peak) and supplied with AC high voltage, while other electrodes are grounded. Moreover, these air-exposed electrodes have been polished, in order to reduce their thickness down to 0.05 mm to prevent them from promoting transition. This value is one order of magnitude lower than the displacement thickness of the boundary layer measured at  $x/c = 10\%$  in the two following experiments. Hot wire anemometry (Dantec Streamline, 90C10 CTA modules, 55P15 probes) has been employed for boundary-layer explorations.

## Transition delay using steady DBD actuation

The study presented in this section is related to 2D boundary-layer stabilization using the plasma actuator in a continuous mode of operation. In this way, a quasi-steady momentum is added to the flow, directly acting on the mean velocity profile of the boundary layer, in such a way that the amplification of the disturbances is impeded and transition can be delayed. For example, this approach has been successfully applied on a flat plate with artificially excited disturbances [9]. In fact, the actuator induces unsteady momentum at the same frequency than the high-voltage signal. This feature is used in the second part of this paper (unsteady actuation). Nevertheless, the effect of the actuator can be considered as quasi-steady in this first experiment, because the operating frequency of the actuator is high compared to the most unstable frequencies of the boundary layer.

## Wind tunnel investigations

In a first step, boundary-layer transition delay is investigated experimentally using one single DBD actuator located at  $x/c = 10\%$  and operated continuously. The angle of attack of the model is set to  $\alpha = 2.5^\circ$  and the experiment has been performed for two different free-stream velocities  $U_\infty = 7$  & 12 m/s. The plasma actuator is supplied with AC high voltage having three different amplitudes  $V_{DBD} = 8.5; 12$  and 17 kV and an operating frequency set to  $f_{DBD} = 2$  kHz. The maximum velocity of the ionic wind induced by the actuator in quiescent air is about 4.5 m/s at the highest voltage amplitude. Figures 3a and 3b present typical results for  $U_\infty = 7$  & 12 m/s. Velocity fluctuations are computed from boundary-layer explorations along the chord, moving the hot-wire probe at a constant distance from the wall, with and without control. The location of the transition is deduced from the fluctuation increase. The natural transition is located at  $x/c \approx 40\%$  for  $U_\infty = 7$  m/s and at  $x/c = 26\%$  for  $U_\infty = 12$  m/s. In all cases, the ignition of the plasma actuator leads to a transition delay. As expected, the transition is shifted progressively downstream when the amplitude of the voltage is increased, since the mechanical effect of the actuator (ionic wind) increases. The maximum transition delays recorded during this experiment are 35 % of the chord for  $U_\infty = 7$  m/s and 20 % of the chord for  $U_\infty = 12$  m/s.

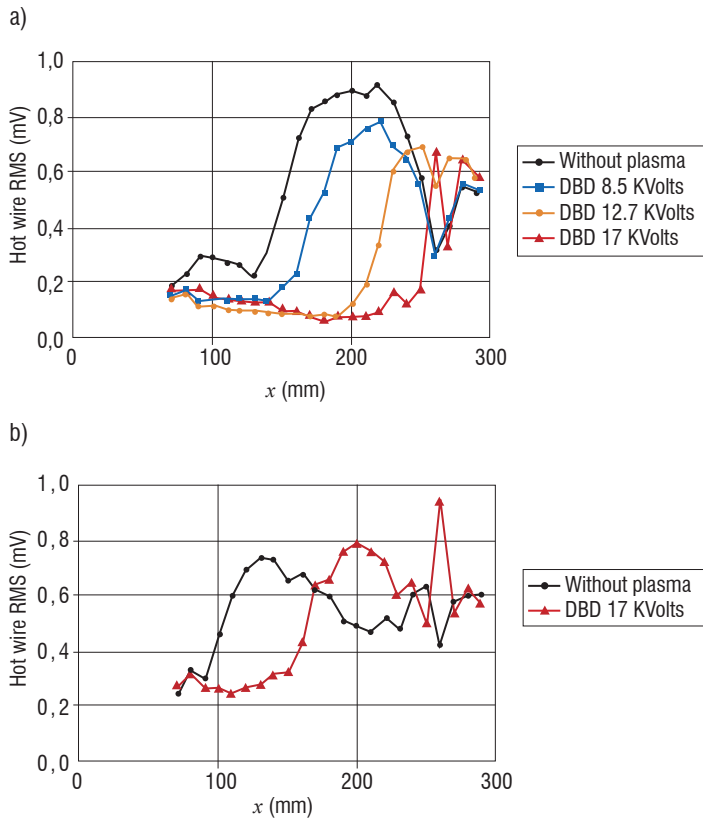


Figure 3 – Transition delay with steady DBD actuation  
a)  $U_\infty = 7$  m/s and b)  $U_\infty = 12$  m/s ( $\alpha = 2.5^\circ$ )

### Numerical investigations

In order to confirm that this transition delay is due to the modification of the mean velocity profile, the control of the boundary layer with steady actuation has been investigated from a numerical point of view. First, boundary-layer computations have been performed for the baseline cases (without plasma) using an Onera code (3C3D, [17]). Then, an artificial ionic wind profile with a simple model (previously described in [20]) has been numerically added at the location of the actuator ( $x/c=10\%$ ) to the mean velocity profiles obtained from these base flow computations, in such a way that the resulting profiles fit the experimental ones. Finally, exact stability computations have been conducted on these modified profiles, using the envelope strategy so as to compute the amplification  $N$ -factor with an Onera code (Castet, [16]).

To describe the laminar-turbulent transition, it is common practice to distinguish three successive processes. The first, taking place close to the leading edge, is the receptivity. It describes the means by which external disturbances (such as free-stream turbulence or noise, as well as wall surface imperfections) excite the eigenmodes of the boundary layer. In the following amplification phase, these eigenmodes develop into periodic waves, which are convected in the streamwise direction. Some of them are exponentially amplified and will trigger transition further downstream. Their evolution is well described by the linear stability theory. When the amplitude of the waves is large, non-linear interactions occur and rapidly lead to turbulence (third step). Within the framework of classical linear stability theory, disturbances are introduced as:

$$q'(x, y, z) = \hat{q}(y) \cdot \exp(-\alpha_i x) \cdot \exp(i(\alpha_r x + \beta z - \omega t)) \quad (1)$$

where  $q'$  is a fluctuation (velocity, pressure or temperature) and  $\hat{q}$  its amplitude function (here  $x$  is perpendicular to the leading edge and  $y$  is

normal to the wall). Considering the spatial theory,  $\alpha = \alpha_i + i\alpha_r$  is the complex wave-number in the  $x$  direction. The spanwise wave-number  $\beta$  and frequency  $\omega$  are real. Introducing expression (1) in the Navier-Stokes equations leads to a system of ordinary differential equations for the amplitude functions. The stability of the flow depends on the value of the imaginary part of the longitudinal component of the amplification vector  $\alpha_i$ . When positive, the flow will be stable; when negative, the perturbation will be amplified until the transition is triggered. To quantify the amplification of disturbances, it is common practice to introduce the so-called  $N$ -factor given by relation (2), where  $A$  is the amplitude of the disturbance at a streamwise position  $x$ . Physically, the  $N$ -factor describes the total amplification rate of small disturbances along the propagation path. Considering a low velocity two-dimensional flow, only two-dimensional waves ( $\beta=0$ ) need to be considered (the  $N$ -factor is simply computed by integrating  $-\alpha_i$  in the streamwise direction), since Squire's theorem states that they are the most relevant ones.

$$N = \ln(A/A_0) = \int_{x_0}^x -\alpha_i(\xi) d\xi \quad (2)$$

As explained previously, an artificial ionic wind profile with a simple model is added to the mean velocity profile of the base flow boundary layer, at the location of the actuator ( $x/c = 10\%$ ). Downstream, the boundary layer is solved by the code with the usual equations. As illustrated in figure 4, three parameters define the ionic wind model:

- $u_{\text{plasma}}$  is the maximum amplitude of the ionic wind profile;
- $y_{\text{max}}$  is the height of this maximum amplitude;
- $y_2$  is the height at which the ionic profile returns to zero.

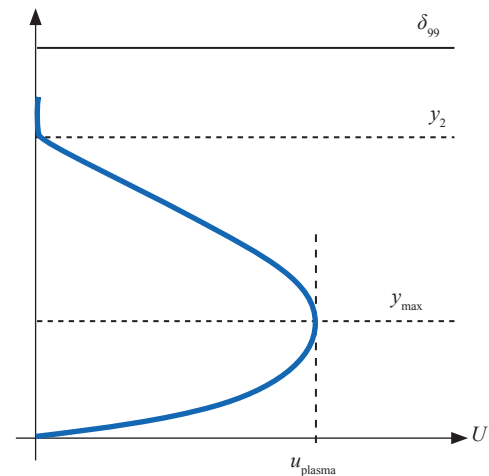
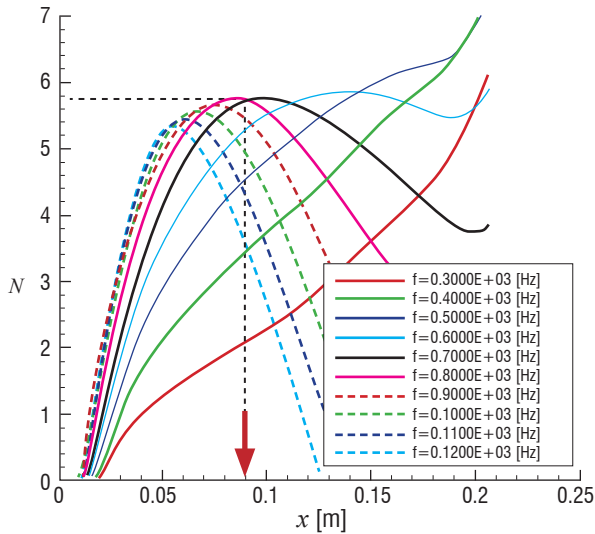


Figure 4 – Simple ionic wind model used to compute the mean velocity profiles of the boundary layer controlled by steady plasma actuation

Typical results of the linear stability analysis are given in figure 5, which presents the evolutions of the  $N$ -factor along the chord of the model for several instability frequencies in the baseline case (a) and for the controlled case (b). The aerodynamic configuration is the same as that for the case presented in figure 3b) with  $U_\infty = 12$  m/s. Since the natural transition location is known from the experiment ( $xt/c \sim 26\%$  or  $xt = 0.09$  m), we can deduce the corresponding transition  $N$ -factor  $N_t = 5.8$ . Then, using this value in the controlled case plot, we can observe that the transition location is shifted downstream ( $xt = 0.22$  m), not far from what has been observed experimentally ( $xt = 0.16$  m). This stability analysis for the controlled case has been performed using ionic wind model parameters that are very close to the experimental values ( $u_{\text{plasma}} = 4$  m/s,  $y_{\text{max}} = 1.2$  mm). The difference between measured

and predicted transition locations could be explained by the relative simplicity of the ionic wind model used here. A new model that takes into account the real spatial force distribution induced by the actuator would provide a better consistency in the results. In conclusion, stability computations as well as experiments show that DBD plasma actuators used in a steady mode have a stabilizing effect on the boundary layer. The modification of the mean velocity profiles is such that the amplification of the disturbances is impeded and transition can be delayed.

a)



b)

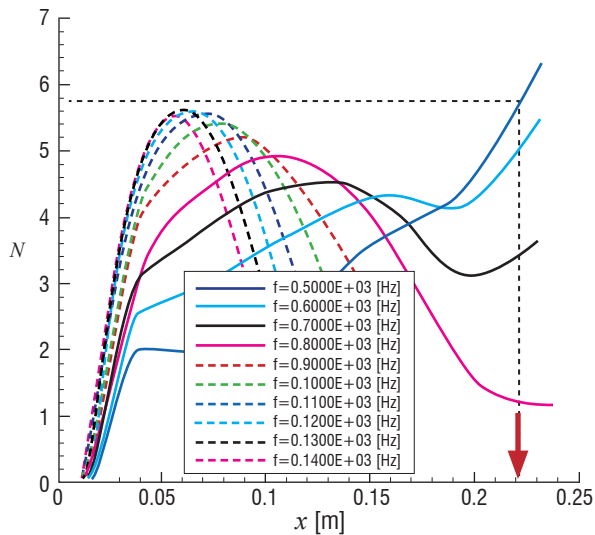


Figure 5 – Evolution of the  $N$ -factor along the chord of the model ( $\alpha = 2.5^\circ$ ,  $U_\infty = 12$  m/s) without control a) and with control b) where  $u_{\text{plasma}} = 4$  m/s and  $y_{\text{max}} = 1.2$  mm

### Transition delay using unsteady DBD actuation

Another way to delay 2D transition is to use unsteadily operated actuators to act (or counteract) directly on the Tollmien-Schlichting waves growing inside the boundary layer and triggering transition. This approach is called Active Wave Cancellation: the goal is to generate an artificial perturbation with an unsteady force production, so as to damp natural TS waves by destructive interference. Transition is delayed because the TS wave amplitude has been reduced locally. Grundmann and Tropea [10] have conducted experiments using this approach on a flat plate. They used a single high-frequency driven DBD actuator with

square wave modulation to generate artificially introduced waves. A sufficiently large difference between the TS wave frequency (modulation frequency) and the operating frequency of the plasma actuator is essential for this operation mode. However, with increasing flow speed, the unstable frequency band will shift to a higher range correspondingly, until a sufficient difference between the carrier frequency and TS wave frequency cannot be maintained anymore. Another possible solution, as suggested by Grundmann in [11], is to make use of the DBD plasma actuator unsteady force production during one cycle of the operating frequency and to directly operate the cancellation actuator at the TS wave frequency. In fact, several experimental [7] [8] and numerical [3] [21] studies have shown that a DBD actuator produces a local unsteady force, mainly due to the different discharge regimes between the positive and the negative half cycles. This phenomenon became clear by analyzing the plasma actuator response electrically [18], or by using optical measurement techniques in the direct vicinity of the plasma region [6]. This asymmetric behavior allows the use of DBD actuators in direct frequency mode. A careful adjustment of the phase relation between the TS waves and the actuator excitation signal can thereby potentially cancel the waves. Thus, the use of an active control system with a closed-loop, which detects the waves and optimizes the actuation, will be necessary.

The experimental set-up used for this study is quite the same as the one presented in the previous section, except that the angle of attack is set to  $\alpha = 2^\circ$  and that the model is outfitted with two DBD actuators, as illustrated in figure 6. The upstream actuator DBD1 ( $x/c = 10\%$ ) serves as a disturbance source to artificially excite a single frequency TS wave train, while DBD2 ( $x/c = 30\%$ ) is utilized as the transition control device.

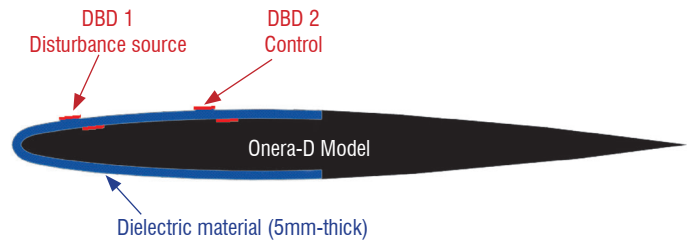


Figure 6 – Experimental set-up for the Active Wave Cancellation study

The experiments have been split into two phases. During an initial testing phase, the feasibility of the direct frequency mode for active wave cancellation had to be verified. In order to do so, a set-up employing a beat frequency approach without the use of a closed-loop controller was chosen, reproducing the experiments of Grundmann and Tropea. This allows for time efficient parameter studies to find appropriate settings and the corresponding attenuation rates. In the second testing phase, transition delay on the wing model has been shown with closed-loop control applied.

### AWC without closed-loop control

For this set of measurements, the excitation frequency at the upstream actuator DBD 1 has been set to a value close to the naturally occurring TS frequencies ( $f_{DBD1} = 250$  Hz). As the artificially excited waves travel downstream, they reach the control actuator (DBD2), which was operated at a slightly shifted frequency ( $f_{DBD2} = 251$  Hz) in order to create a beat frequency with the two signals due to the continuously changing phase relation. Some typical results from these experiments are presented in figure 7 for a free-stream velocity of  $U_\infty = 7$  m/s.

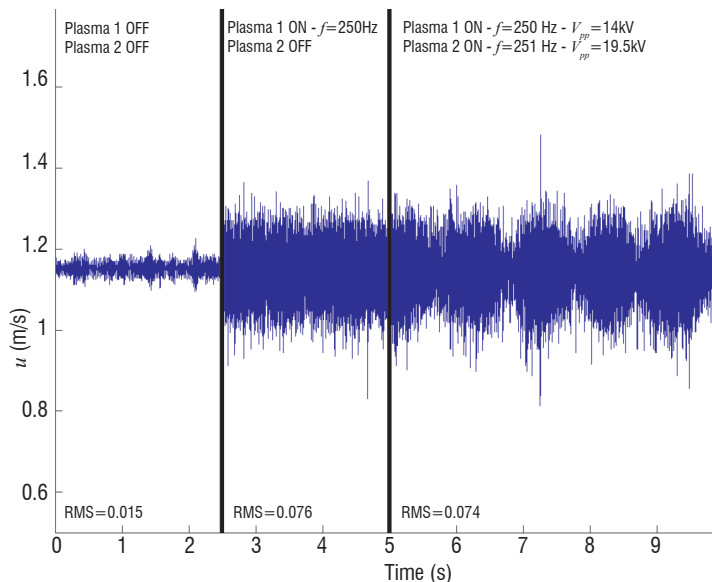


Figure 7 – Time trace of  $u$  velocity component given by a hot-wire probe located inside the boundary layer at  $x/c = 40\%$  for the base flow (left), with excitation (center) and with excitation and control (right)

The hot wire measurements shown were taken at  $x/c = 40\%$  inside the boundary layer, at a wall-normal distance of  $y = 0.4$  mm. The base flow case (left part of the plot) shows a low fluctuation level within the hot-wire signal of 0.015 m/s. With excitation (middle part of the plot), this disturbance level is raised to 0.076 m/s. Applying the control (right part of the plot), a slow oscillation of the amplitude of the TS waves develops farther downstream from the second actuator, with a maximum amplitude above that of the unaffected waves (amplification) and minimum amplitude below the unaffected wave (damping), resulting in an almost unchanged RMS-value of 0.074 m/s in this case. Figure 8 shows a time trace of the excited TS wave signal with smaller time scale (dashed line) compared to the base flow case (solid line), revealing that a clean TS wave train has been produced by DBD1. Two important results emerge from these experiments. First of all, the unsteady momentum production of the plasma actuator can be utilized to excite TS waves, if applied at the appropriate position, amplitude and a frequency that the flow is susceptible to. Secondly and most importantly, the direct frequency approach for flow control proved to be applicable and can be utilized for active wave cancellation.

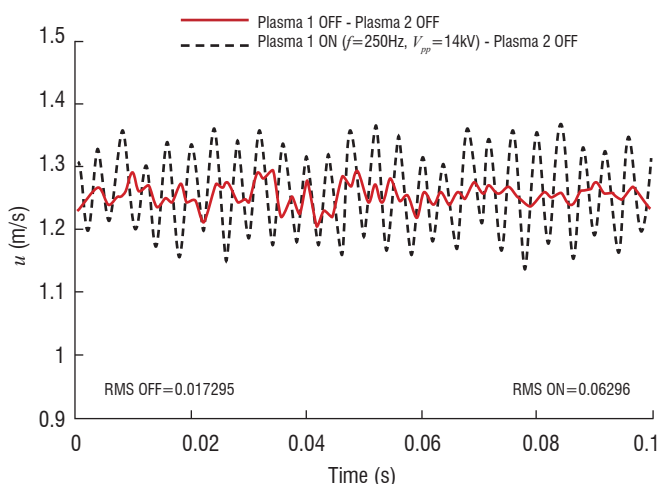


Figure 8 – Time trace of the  $u$  velocity component given by a hot-wire probe located inside the boundary layer at  $x/c = 40\%$  for the base flow (solid line) and with DBD1 turned on (dashed line)

## AWC using closed-loop control

In order to have a permanent optimized phase shift between the TS waves generated by DBD1 and the controlling unsteady force induced by DBD2, a robust extremum-seeking control algorithm has been used. This algorithm, which has previously been successfully applied for flow control purposes [1], was supplied by the TU Berlin. The system utilizes the signal of a stationary hot wire probe ( $x/c = 40\%$ ,  $y = 0.2$  mm) as an error sensor to automatically optimize the control function. This control algorithm runs on a dSPACE real-time processing unit. Due to its robustness this algorithm is well suited to control artificially excited, single-frequency TS waves. By slowly and periodically deflecting the system out of its current operating point (perturbation), the gradient  $f'$  of the error signal is determined according to a change of the controlled variable, which in this case is the phase shift. The phase relation between the TS wave train and the flow structures created by the plasma actuator is then continuously adapted along this gradient, which drives the system into a minimum.

Following the promising beat frequency experiments, closed-loop control has been applied in order to show the transition delay using the direct frequency approach. The free-stream velocity and the angle of attack remain at  $U_\infty = 7$  m/s and  $\alpha = 2^\circ$  respectively. A spectral analysis of the stationary hot-wire signal reveals the frequency content of the flow, as shown in figure 9. The power spectral density is plotted in dB/Hz over frequency at a wall-normal position of  $y = 0.2$  mm. In the base flow case (DBD1 off, DBD2 off) two frequency peaks, one at 250 Hz and a wider peak around 340 Hz, are prominent. These frequencies represent the naturally occurring TS waves present in the boundary layer for the given flow situation. However, as has been shown with linear stability analysis, well described in [13], frequencies around 340 Hz are damped downstream of DBD2, with the limit for the unstable frequency band being about 300 Hz. A frequency sweep in the unstable range revealed that an excitation at 280 Hz leads to the cleanest TS wave signal at the location of the error sensor. Consequently it was decided to use this frequency for the subsequent AWC experiments. Figure 9 shows that introducing the excitation at 10 % of the chord (DBD1 on, DBD2 off) produces the expected peak around 280 Hz, as well as an overall increase in the turbulence level as transition is being promoted. This increase is visible at the error sensor, since its location is close to the point of transition for the excited case ( $\sim 47\%$  of the chord). Applying the control (DBD1 on, DBD2 on) the TS peak at 280 Hz can be reduced by about one order of magnitude. This effect is accompanied by a decreased overall turbulence level.

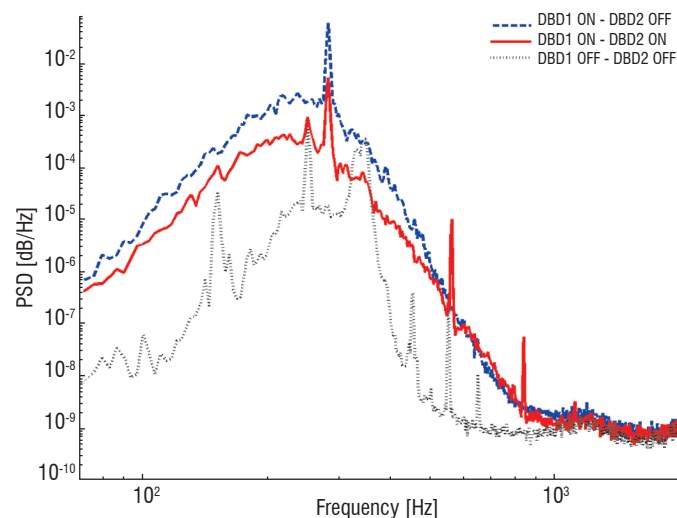


Figure 9 – Spectral analysis of the error sensor signal ( $x/c = 40\%$ ,  $U_\infty = 7$  m/s) for the base flow (DBD1 off, DBD2 off), with excitation (DBD1 on, DBD2 off) and with closed-loop control (DBD1 on, DBD2 on)

Figure 10 depicts a typical result of the transition delay studies. The RMS-value of the longitudinal velocity fluctuations recorded at various downstream locations at a constant distance above the wall within the boundary layer is plotted. The dark blue curve ( $\diamond$ ) represents the natural transition case with the onset of transition at about 60% of the chord, *i.e.*, neither the disturbance source nor the control actuator is operating. Turning on the disturbance source, the TS wave amplitude is significantly increased at  $f = 280$  Hz, which moves the transition region upstream to about 40% of the chord ( $\square$ ). Then, with the control system active, the transition region can be shifted downstream significantly by about 10% of the chord length ( $\circ$ ).

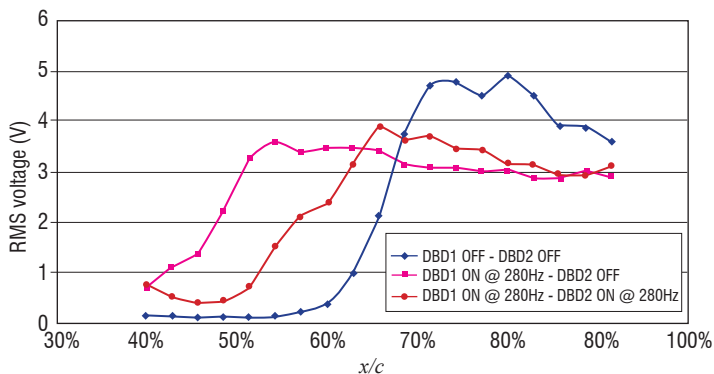


Figure 10 – RMS value of a hot-wire signal along the chord of the airfoil for the base flow, with excitation and with closed-loop control ( $\alpha = 2^\circ$ ,  $U_\infty = 7$  m/s)

Even though the unsteadiness of the force production of DBD plasma actuators is used in this work to conduct active wave cancellation, it cannot be neglected that a net force is produced, which modifies the mean flow, *i.e.*, the boundary-layer velocity profile. This modification can by itself lead to a stabilization of the boundary layer, as presented in the previous text section, hence the delay in the transition. Complementary measurements have been carried out in order to exclude possible boundary-layer stabilization due to continuous addition of momentum. To quantify this effect, the momentum generation of DBD2 has been measured in quiescent air, using Pitot-tube measurements. The maximum achievable velocity, 10 mm downstream of the active electrode, was determined to be  $\sim 0.6$  m/s at the prescribed plasma frequency of 280 Hz using this electrode configuration, dielectric material and thickness. In order to deactivate the active wave cancellation and to quantify the effect of a pure momentum addition of this magnitude, the recorded average wall-jet velocity has been reproduced at a plasma frequency of 1 kHz using DBD2. This frequency is located well outside the unstable frequency range and is assumed not to have any destabilizing effect on the boundary layer. The transition delay due to continuous momentum addition is small compared to the effect of the active wave cancellation and is of the order of 1-2 % of the chord length. For higher Reynolds numbers, it can be assumed that this effect will be reduced even further. This experiment proves that the achieved results can

clearly be attributed to the unsteady force production of the DBD plasma actuator and are not the result of a modified mean flow.

The same experiment has been conducted with a higher free-stream velocity  $U_\infty = 20$  m/s. The angle of attack has been slightly reduced to  $\alpha = 1.5^\circ$ , in order to have the natural transition location near  $x/c = 60\%$ , as for the previous case. This time the frequency of the disturbance source is set to  $f_{DBD1} = 1$  kHz, which is close to the frequency of the most unstable perturbations for this aerodynamic configuration. The changes in the velocity fluctuation along the chord, shown in figure 11, prove that transition delay has been achieved (4% of the chord) using a DBD plasma actuator with a closed-loop control system.

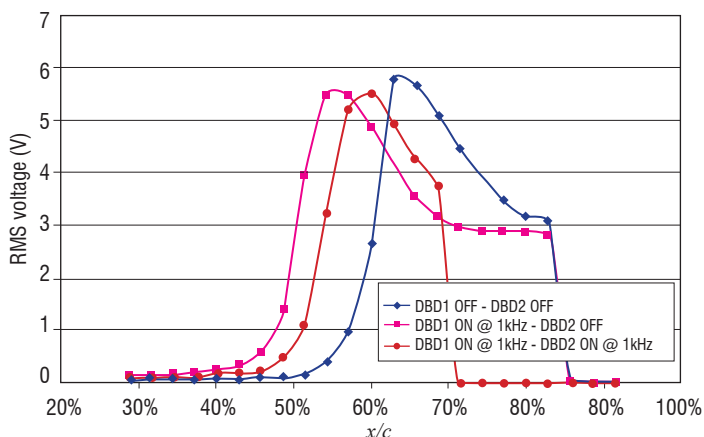


Figure 11 – RMS value of a hot-wire signal along the chord of the airfoil for the base flow, with excitation and with closed-loop control ( $\alpha = 1.5^\circ$ ,  $U_\infty = 20$  m/s)

## Conclusion

In this study, the ability of DBD plasma actuators to delay 2D boundary-layer transition has been assessed, by means of either steady or unsteady actuation. On the one hand, wind tunnel investigations together with linear stability analysis have shown that a DBD actuator used in a steady mode has a stabilizing effect on the boundary layer. The modification of the mean velocity profiles is such that the amplification of the disturbances is impeded and transition can be delayed. A maximum transition delay of about 35 % of the chord has been achieved for low free-stream velocity ( $U_\infty = 7$  m/s). On the other hand, an experiment has been performed using the unsteady force produced by the DBD actuator to achieve Active Wave Cancellation in direct frequency mode. With the help of a closed loop control system, a significant transition delay has been achieved, by damping artificial TS waves for free-stream velocities up to  $U_\infty = 20$  m/s ■

## References

- [1] R. BECKER, R. KING, R. PETZ and W. NITSCHKE – *Adaptive Closed-Loop Separation Control on a High-Lift Configuration using Extremum Seeking*. AIAA Journal, vol. 45, pp. 1382-1392, 2007.
- [2] N. BENARD and E. MOREAU – *EHD Force and Electric Wind Produced by Plasma Actuators Used for Airflow Control*. Proc. of the 6<sup>th</sup> AIAA Flow Control Conference, AIAA Paper 2012-3136, 2012.
- [3] J.P. BOEUF, Y. LAGMICH and L. C. PITCHFORD – *Contribution of Positive and Negative Ions to the Electrohydrodynamic Force in a Dielectric Barrier Discharge Operating in Air*. Journal of Applied Physics, vol. 106-023115, 2009.
- [4] D. CARUANA, P. BARRICAU, P. HARDY, J.P. CAMBRONNE and A. BELINGER – *The Plasma Synthetic Jet Actuator. Aero-Thermodynamic Characterization and First Flow Control Applications*. Proc. of the 47<sup>th</sup> AIAA Aerospace Sciences Meeting, AIAA Paper 2009-1307, 2009.
- [5] T.C. CORKE, C.L. ENLOE and S.P. WILKINSON – *Dielectric Barrier Discharge Plasma Actuators for Flow Control*. Annu Rev Fluid Mech, vol. 42, pp. 505-529, 2010.
- [6] C.L. ENLOE, T.E. McLAUGHLIN, R.D. VANDYKEN, K.D. KACHNER, E.J. JUMPER and T.C. CORKE – *Mechanisms and Responses of a Single Dielectric Barrier Plasma Actuator: Plasma Morphology*. AIAA Journal, vol. 42, n° 3, pp. 595-605, 2004.
- [7] M. FORTE, L. LEGER, J. PONS, E. MOREAU and G. TOUCHARD – *Plasma Actuators for Airflow Control: Measurement of the Non-Stationary Induced Flow Velocity*. Journal of Electrostatics, vol. 63, n° 6-10, pp. 929-936, 2005.
- [8] M. FORTE, J. JOLIBOIS, J. PONS, E. MOREAU, G. TOUCHARD and M. CAZALENS – *Optimization of a Dielectric Barrier Discharge Actuator by Stationary and Non-Stationary Measurements of the Induced Flow Velocity: Application to Airflow Control*. Experiments in Fluids, vol. 43, pp. 917-928, 2007.
- [9] S. GRUNDMANN and C. TROPEA – *Experimental Transition Delay Using Glow-Discharge Plasma Actuators*. Experiments in Fluids, vol. 42, n° 4, pp. 653-657, 2007.
- [10] S. GRUNDMANN and C. TROPEA – *Active Cancellation of Artificially Introduced Tollmien-Schlichting Waves Using Plasma Actuators*. Experiments in Fluids, vol. 44, n° 5, pp. 795-806, 2008.
- [11] S. GRUNDMANN – *Transition Control Using Dielectric Barrier Discharge Actuators*. Ph.D. Dissertation, Institute for Fluid Mechanics and Aerodynamics, Technische Universität Darmstadt, 2008.
- [12] P. HARDY, P. BARRICAU, D. CARUANA, C. GLEYZES, A. BELINGER and J.P. CAMBRONNE – *Plasma Synthetic Jet for Flow Control*. Proceedings of the 40<sup>th</sup> AIAA Fluid Dynamics Conference and Exhibit, AIAA Paper 2010-5103, 2010.
- [13] A. KURZ, C. TROPEA, S. GRUNDMANN, M. FORTE, O. VERMEERSCH, A. SERAUDIE, D. ARNAL, N. GOLDIN and R. KING – *Transition Delay Using DBD Plasma Actuators in Direct Frequency Mode*. Proceedings of the 6<sup>th</sup> AIAA Flow Control Conference, AIAA Paper 2012-2945, 2012.
- [14] L. LEGER, E. MOREAU and G. TOUCHARD – *Electrohydrodynamic Airflow Control Along a Flat Plate by a DC Surface Corona Discharge – Velocity Profile and Wall Pressure Measurements*. Proceedings of the 1<sup>st</sup> AIAA Flow Control Conference, AIAA Paper 2002-2833, 2002.
- [15] E. MOREAU – *Airflow Control by Non-Thermal Plasma Actuators*. Journal of Physics D: Applied Physics, vol. 40, pp. 605-636, 2007.
- [16] J. PERRAUD – *Description et mode d'emploi du code CASTET*. Technical Report Onera/DERAT RT n° 124/5118.32, 1997.
- [17] J. PERRAUD, O. VERMEERSCH and R. HOUEVILLE – *Descriptif et mode d'emploi du code 3C3D*. Technical Report Onera RT 1/18325 DMAE, 2011.
- [18] J. PONS, E. MOREAU and G. TOUCHARD – *Asymmetric Surface Dielectric Barrier Discharge in Air at Atmospheric Pressure: Electrical Properties and Induced Airflow Characteristics*. Journal of Physics D: Applied Physics, vol. 38, pp. 3635-3642, 2005.
- [19] J. R. ROTH, D. M. SHERMAN and S. P. WILKINSON – *Boundary Layer Flow Control with a One Atmosphere Uniform Glow Discharge Surface Plasma*. Proceedings of the 36<sup>th</sup> AIAA Aerospace Sciences Meeting and Exhibit, AIAA Paper 98-0328, 1998.
- [20] A. SERAUDIE, O. VERMEERSCH and D. ARNAL – *DBD Plasma Actuator Effect on a 2D Model Laminar Boundary Layer. Transition Delay under Ionic Wind Effect*. Proc. of the 29<sup>th</sup> AIAA Applied Aerodynamics Conference, AIAA Paper 2011-3515, 2011.
- [21] T. UNFER and J. P. BOEUF – *Modeling and Comparison of Sinusoidal and Nanosecond Pulsed Surface Dielectric Barrier Discharges for Flow Control*. Plasma Physics and Controlled Fusion, vol. 52, n° 12-124019, 2010.

## Acronyms

Active Wave Cancellation (AWC)  
Dielectric Barrier Discharge (DBD)  
Plasma Synthetic Jet (PSJ)  
Root Mean Square (RMS)  
Tollmien Schlichting (TS)



**Armin Kurz** graduated in 2003 from the University of Arizona where he obtained his Masters degree in Aerospace Engineering. Since 2008, he works as a doctoral student in the Drag and Circulation Control (DCC) Group of the Center of Smart Interfaces in Darmstadt. His current activities involve boundary-layer transition control with the use of plasma actuators.



**Sven Grundmann** obtained his Degree in Mechanical Engineering from the Technische Universität Darmstadt in 2003 and received his PhD in 2008 from the same institution. After a postdoctoral position in 2009 at the Stanford University in the Department of Flow Physics and Computational Engineering, he finally joined the Center of Smart Interfaces (CSI) and the Technische Universität Darmstadt in 2010. As a young research group leader, his research interests include drag and circulation control and magnetic resonance imaging for fluid mechanics.



**Cameron Tropea** graduated from the University of Toronto in Engineering Sciences, followed by a Masters degree in Mechanical Engineering (1977). He completed his Dr.-Ing. in Civil Engineering at the Technical University of Karlsruhe (1982) and his Habilitation in Fluid Mechanics at the University of Erlangen-Nürnberg (1991) where he was appointed as Professor of Fluid Mechanics until 1997. This was followed by an appointment to his current chair of Fluid Mechanics and Aerodynamics at the Technische Universität Darmstadt. Currently Editor-in-Chief of the Springer journal Experiments in Fluids, he is also the Director of Center of Smart Interfaces (CSI) since 2007. His research interests include Optical Measurement Techniques in Fluid Mechanics, Interfacial Transport Phenomena, Atomization and Spray Processes and Instationary Aerodynamics.



**Maxime Forte** graduated from École Nationale Supérieure de Mécanique et d'Aérotechnique (ENSMA - French engineering school specialized in space and aeronautics) in 2004 and received his PhD in Fluid Mechanics from the University of Poitiers in 2007. He joined Onera in 2010 and works as a research scientist in the Aerodynamics and Energetics Modeling Department in Toulouse. His research interests include experimental investigations on boundary-layer transition (flow control, tripping criteria and new devices for transition detection).



**Alain Seraudie** joined Onera in 1972 and worked as a research assistant specialized in experimental investigations on transonic flows. Graduated from Conservatoire National des Arts et Métiers (CNAM) in 1982, he then worked as a research scientist in one of the first cryogenic, pressurized and transonic wind tunnel in Europe. In the early 2000's, he joined the research unit "Transition and Instability" led by D. Arnal and started working experimentally on boundary-layer transition issues until he retired in 2011.



**Olivier Vermeersch** graduated from École Nationale Supérieure de Mécanique et d'Aérotechnique (ENSMA - French engineering school specialized in space and aeronautics) in 2006 and received his PhD in Fluid Mechanics from the University of Toulouse in 2009. Since then, he has worked as a research scientist in the Aerodynamics and Energetics Modeling Department of Onera. His research interests include boundary-layer stability computations and control of the laminar/turbulent transition with different kinds of actuation (micro-sized roughnesses, plasma actuators).



**Daniel Arnal** is a graduate from of Ecole Nationale Supérieure de Mécanique et Aérotechnique (ENSMA) in Poitiers, France. He received his PhD in 1976 from Onera Toulouse. He is working for more than 30 years on the topics related to laminar-turbulent transition (hydrodynamic instability, transition prediction, laminar flow control). In 1998, he became the Head of the research unit "Transition and Instability" in the Aerodynamics and Energetics Modeling Department at Onera Toulouse. He published approximately 150 archival journals or meeting papers.



**Nikolas Goldin** obtained his degree in Applied Mathematics from the Technische Universität Berlin in 2006. He completed his Dr.-Ing. in Control Engineering at the same institution in 2013. He is currently with DFG SFB 1029 at Technische Universität Berlin as a postdoctoral researcher. His research interests include drag reduction by flow control, biomimetics and flow control in gas turbines.



**Rudibert King** received his Dr.-Ing. from University of Stuttgart in 1988 and completed his habilitation in 1993. In 1993, he joined the University of Siegen as a Professor for Simulation Techniques. He moved to Berlin where he was appointed to Professor for Measurement and Control at the Technische Universität Berlin in 1995. His research interests include process control of chemical and biological systems, flow control, automatic modelling of reaction systems and control in uncertain systems.